

## Quantification of Cerebral Arteriole Oxygenation in Human Brain by qBOLD Technique

Xiang He<sup>1</sup>, Chan-Hong Moon<sup>1</sup>, Serter Gumus<sup>1</sup>, Ayaz Aghayev<sup>1</sup>, JinHong Wang<sup>1</sup>, Dmitriy A Yablonskiy<sup>2</sup>, and Kyongtae Ty Bae<sup>1</sup>

<sup>1</sup>Department of Radiology, University of Pittsburgh, Pittsburgh, PA, United States, <sup>2</sup>Mallinckrodt Institute of Radiology, Washington University in St Louis, St Louis, Missouri, United States

**Introduction:** Direct measurement of oxygen saturation,  $PO_2$ , in brain cortex arteries, arterioles and capillaries is of great physiological importance, as the arterioles and capillaries deliver oxygen to the brain tissue. Early work in the 1970's by Duling and Berne used microcathodes in hamster model to demonstrate the existence of oxygen diffusion from precapillary arterioles (8 $\mu$  to 100 $\mu$  in diameter) (1). Recent works in rodent models by the Vovenko group using oxygen microelectrode (2), the Boas group (using OCTOPuS with Oxyphor R2 dye) (3), and the Kim group (using Clark-type oxygen probe) (4) measured microvascular  $PO_2$  in the baseline state and under evoked neural stimulation. These studies demonstrated that the increase in arterial  $PO_2$  contributes to hyper-oxygenation of tissue and also to signal changes in BOLD fMRI. While a non-invasive MRI-based T2 and T2\* approach has also been used by Kim's group in a rat model,  $PO_2$  quantification accuracy was low due to a limited number of decay profile sampling points, which were often acquired at different times. In this study, we adopt the ASL-qBOLD technique (5) to measure the precapillary arteriole blood oxygenation in the human brain in both baseline and activated states.

**Methods:** The ASL-qBOLD is a hybrid of FAIR-based (flow-sensitive alternation inversion recovery) pulsed ASL, and GESSE (gradient echo sampling of spin echo) technique (7) to study T2\* properties of ASL water signal. To improve robustness of the ASL acquisition, background suppression and QUIPPS II techniques were implemented. Data analysis was based on the model of T2\* decay of the arteriole blood MR signal that is governed by its intrinsic  $R2^*=1/T2^*$  decay and the "powder effect" (6):

$$s_i(t) = [\pi/(3 \cdot |\delta\omega \cdot t|)]^{1/2} \exp(-R2^* \cdot t - i \cdot \delta\omega \cdot t/2) \cdot [C(|3\delta\omega \cdot t/2|^{1/2}) - i \cdot \text{sign}(t) \cdot S(|3\delta\omega \cdot t/2|^{1/2})], \quad (1)$$

Where  $C(\cdot)$  and  $S(\cdot)$  are Fresnel cosine and sine integral functions, respectively;  $\delta\omega$  relates to blood Hct and oxygen saturation level (7,8). Eq. 1 assumes a uniform orientation of small arteries and arterioles, but may not apply to large arteries. All experiments were performed on a 3T Siemens Trio scanner using a 32 channel head RF coil. MR parameters for ASL-qBOLD were: labeling time (TI) of 600 ms, post-labeling saturation pulse train at 300 ms before image acquisition; sampling matrix of 64x48 with voxel size of 4x4x8 mm<sup>3</sup>; TR of 2000 ms; echo train length of 57 with 2.36 ms echo spacing (spin echo of 46 ms at 6<sup>th</sup> gradient echo). K-space data of control and labeling images were acquired in an interleaved mode. Acquisition time for a complete set of ASL images was three minutes. Six sessions were performed on four healthy volunteer subjects in baseline state and under visual stimulation with a flashing checkerboard paradigm.

### Results & Discussions:

To investigate the composition of arterial ASL signal, we acquired two baseline data sets with and without QUIPPS mechanism. Fig. 1 (left panel) shows images of ASL signal intensity at spin echo time. T2\* decay profile of ASL water signal with QUIPPS (red circles, averaged across GM ROI), and the difference between two ASL signals (blue squares) are also presented. The difference between ASL signals corresponds to the ASL water signal that originates mainly in large feeding arteries. The estimated apparent T2\* for the large artery ASL water was 91 ms, compared to the estimated T2\* for arteriole ASL signal of 51 ms. The origin of this later-arriving labeled blood was independently confirmed in a separate study with total labeling time (TI) of 300 ms without QUIPPS. The estimated apparent T2\* for this ASL water was 87 ms. A slightly decrease of apparent arteriole T2\* decay time constant was observed when TI was varied at 500, 600 and 700 ms. The estimated apparent T2\* for arteriole blood (with QUIPPS) was 48.1 ms, 42.3 ms and 37.3 ms, respectively. This may suggest that blood in small arteries and arterioles continuously loses oxygen before reaching the capillary bed, in agreement with (1).

To estimate the exact arteriole  $PO_2$  of the labeling bolus, T2\* evolution profile was fitted to the intravascular signal model as described in Eq. 1. In all studies, the model was in good agreement with the measured T2\* data. The estimated mean baseline arteriole blood  $PO_2$  across six studies was  $86.9 \pm 3.4\%$  which is consistent with rodent model studies using invasive approaches (2-4). Fig. 2 shows T2\* decay profile in primary visual cortex ROI before (red squares), during (green circles) and after (blue diamonds) visual stimulation. T2\* decay time constant was not significantly changed. The mean decrease in arteriole blood  $PO_2$  was 1.3% during visual stimulation, contrary to direct observations (4). It is known that at a fixed position within arterial vasculature, blood oxygenation increases slightly during stimulation. However, this effect may be compensated by the blood velocity increases during activation, which pushes the labeling arterial bolus further down the vasculature tree (less  $PO_2$ ). **In Conclusion**, we have demonstrated that measuring T2\* using ASL-qBOLD technique allows the differentiation of blood signal originated in different branches of the arterial tree.

**References:** (1) Duling, et al., CirRes 1970; 27:669. (2) Vovenko, PfugersArch 1999; 437:617. (3) Yasen, et al., JCBFM 2011;31:1051. (4) Vazquez, et al., JCBFM 2010;30:428. (5) He, et al., MRM 2011., online. (6) Sukstanskii & Yablonskiy, JMR 2004; 167:56. (7) He & Yablonskiy, MRM 2007; 57:115. (8) Yablonskiy & Haacke, MRM 1994; 32:749.

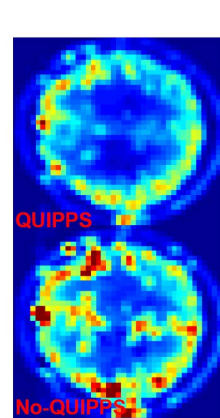


Fig. 1

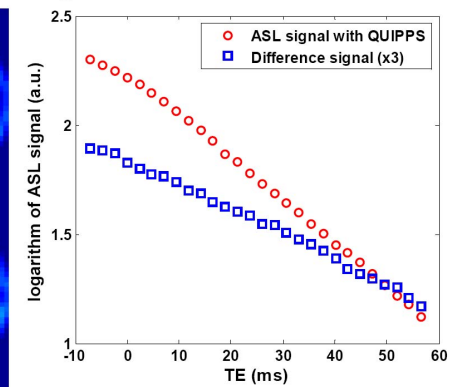


FIG. 2

